HHS Public Access

Author manuscript

Cell Metab. Author manuscript; available in PMC 2016 May 05.

Published in final edited form as:

Cell Metab. 2015 May 5; 21(5): 706–717. doi:10.1016/j.cmet.2015.04.002.

SIRT1-mediated eNAMPT secretion from adipose tissue regulates hypothalamic NAD+ and function in mice

Myeong Jin Yoon[1,5], **Mitsukuni Yoshida**[1,5], **Sean Johnson**[1,5], **Akiko Takikawa**[2], **Isao Usui**[2], **Kazuyuki Tobe**[2], **Takashi Nakagawa**[3], **Jun Yoshino**[4], and **Shin-ichiro Imai**[1,*]

[1]Department of Developmental Biology, Washington University School of Medicine, St. Louis, MO 63110

[2]The First Department of Internal Medicine, Graduate School of Medicine and Pharmaceutical Science for Research, University of Toyama, Toyama, Japan

[3]Frontier Research Core for Life Sciences, University of Toyama, Toyama, Japan

[4]Division of Geriatrics and Nutritional Science, Department of Medicine, Washington University School of Medicine, St. Louis, MO 63110

SUMMARY

Nicotinamide phosphoribosyltransferase (NAMPT), the key NAD^+ biosynthetic enzyme, has two different forms, intra- and extracellular (iNAMPT and eNAMPT), in mammals. However, the significance of eNAMPT secretion remains unclear. Here we demonstrate that deacetylation of iNAMPT by the mammalian NAD^+-dependent deacetylase SIRT1 predisposes the protein to secretion in adipocytes. NAMPT mutants reveal that SIRT1 deacetylates lysine 53 and enhances eNAMPT activity and secretion. Adipose tissue-specific *Nampt* knockout and knockin (ANKO and ANKI) mice show reciprocal changes in circulating eNAMPT, affecting hypothalamic NAD^+/SIRT1 signaling and physical activity accordingly. The defect in physical activity observed in ANKO mice is ameliorated by nicotinamide mononucleotide (NMN). Furthermore, administration of a NAMPT-neutralizing antibody decreases hypothalamic NAD^+ production, and treating *ex vivo* hypothalamic explants with purified eNAMPT enhances NAD^+, SIRT1 activity, and neural activation. Thus, our findings indicate a critical role of adipose tissue as a modulator for the regulation of NAD^+ biosynthesis at a systemic level.

*Correspondence: Shin-ichiro Imai, M.D., Ph.D., Professor, Department of Developmental Biology, Washington University School of Medicine, Campus Box 8103, 660 South Euclid Avenue, St. Louis, MO 63110, Tel: (314) 362-7228 Fax: (314) 362-7058 imaishin@wustl.edu.

[5]These authors contributed equally to this work

Author Contributions

S.I. conceived and supervised the entire study. M.J.Y., M.Y., S.J., J.Y., and S.I. designed the experiments. M.J.Y performed most of the experiments related to Figures 1–5, M.Y. and S.J. performed experiments related to Figures 2D and 6–7, and J.Y. performed the experiments related to Figure 5. A.T., I.U., K.T., and T.N. produced and provided *AT-Sirt1*$^{-/-}$ and control mice. M.J.Y., M.Y., S.J., J.Y., and S.I analyzed the data and wrote the manuscript.

INTRODUCTION

The biosynthesis of nicotinamide adenine dinucleotide (NAD^+), an essential coenzyme and important currency for cellular energy metabolism, plays a critical role in the regulation of diverse biological processes through key NAD^+-consuming mediators, including poly-ADP-ribose polymerases (PARPs), CD38/157 ectoenzymes, and sirtuins (Stein and Imai, 2012). NAD^+ can be synthesized from four different substrates: nicotinamide, nicotinic acid, tryptophan, and nicotinamide riboside (NR) (Houtkooper et al., 2010; Imai and Guarente, 2014). Among them, nicotinamide is predominantly used to synthesize NAD^+ in mammals (Stein and Imai, 2012). Starting from nicotinamide, NAD^+ biosynthesis is catalyzed by two key enzymes: nicotinamide phosphoribosyltransferase (NAMPT) and nicotinamide mononucleotide adenylyltransferase (NMNAT) (Garten et al., 2009; Imai, 2009; Imai and Guarente, 2014). NAMPT, the rate-limiting enzyme in this NAD^+ biosynthetic pathway, catalyzes the conversion of nicotinamide and 5′-phosphoribosyl-pyrophosphate (PRPP) to nicotinamide mononucleotide (NMN), a key NAD^+ intermediate. NMN, in turn, is adenylated by NMNAT to generate NAD^+.

NAMPT is a unique enzyme that has an ancient origin and an interesting research history (Garten et al., 2009; Imai, 2009). NAMPT was originally identified as the product of the gene that confers the capability of synthesizing NAD^+ from nicotinamide, called *NadV*, in *Haemophilus ducreyi* (Martin et al., 2001). Surprisingly, a set of genes encoding NAMPT and NMNAT homologues has even been found in some bacteriophages (Miller et al., 2003). The biochemical and structural features of NAMPT have been extensively studied by our and other groups, clearly demonstrating that this protein belongs to a dimeric class of type II phosphoribosyltransferases (Khan et al., 2006; Revollo et al., 2004; Rongvaux et al., 2002; Wang et al., 2006). Interestingly, NAMPT has two different forms in mammals: intra- and extracellular NAMPT (iNAMPT and eNAMPT, respectively) (Revollo et al., 2007). eNAMPT was previously identified as pre-B cell colony-enhancing factor (PBEF), a presumptive cytokine that enhanced the maturation of B cell precursors, and as visfatin, a visceral fat-derived adipokine once proposed to exert an insulin-mimetic function by binding to the insulin receptor (Fukuhara et al., 2005, 2007; Garten et al., 2009; Imai, 2009; Samal et al., 1994). Neither function of PBEF nor visfatin has been reconfirmed to date. Our previous study has clearly demonstrated that NAMPT functions as an intra- and extracellular NAD^+ biosynthetic enzyme and that eNAMPT does not exert insulin-mimetic effects, either *in vitro* or *in vivo* (Revollo et al., 2007). However, the physiological relevance and function of eNAMPT has still been controversial, and whether eNAMPT secretion is actively regulated has been of significant debate. Here we demonstrate that eNAMPT secretion is regulated by SIRT1-mediated deacetylation in adipose tissue and also that eNAMPT secreted by adipose tissue plays an important role in the maintenance of hypothalamic NAD^+ production and its function *in vivo*.

RESULTS

Acetylation levels of iNAMPT affect the secretion of eNAMPT

Fully differentiated brown and white adipocytes secrete eNAMPT, which has 2–4-fold higher enzymatic activity than iNAMPT (Revollo et al., 2007). We speculated that a post-

translational modification was likely responsible for this altered enzymatic activity and the secretion of eNAMPT. Analysis of its post-translational modification, including acetylation and ADP-ribosylation, revealed that iNAMPT was acetylated in brown and white adipose tissue (BAT and WAT, respectively) (Figure 1A). Interestingly, acetylation levels of iNAMPT decreased by ~50% in response to 48-hr fasting (Figure 1A). To further assess the effect of NAMPT acetylation on its function and secretion, we examined differentiated HIB-1B brown adipocytes, which express a very high level of iNAMPT and secrete eNAMPT into culture supernatants (Revollo et al., 2007). In their cell extracts, relatively low levels of acetylated iNAMPT were detected (Figure 1B, lane M). Acetylation levels significantly increased when treating cells with trichostatin A (TSA) and nicotinamide, inhibitors of class I and II deacetylases and class III NAD^+-dependent deacetylases, respectively (Figure 1B, right two T+N lanes). In this condition, iNAMPT protein levels did not change in cell extracts, whereas secreted eNAMPT protein levels in culture supernatants decreased by ~60% (Figure 1C), implicating that the acetylation status of iNAMPT might predispose the protein to secretion. Because fasting decreased acetylation levels of iNAMPT in adipose tissue, we examined the effects of low glucose in media on iNAMPT acetylation and eNAMPT secretion in HIB-1B cells. Detection of changes in iNAMPT acetylation turned out to be technically difficult due to low basal levels of acetylated iNAMPT in HIB-1B cells. Nonetheless, lowering glucose dramatically enhanced eNAMPT secretion 3.5–5.5-fold in differentiated HIB-1B cells and 3T3-L1 white adipocytes (Figure 1D). Furthermore, nicotinamide completely inhibited the enhancement of eNAMPT secretion by low glucose (Figure 1D), suggesting that nicotinamide-sensitive sirtuin family members might be responsible for low glucose-induced enhancement of eNAMPT secretion.

SIRT1 regulates eNAMPT secretion by physically interacting with and deacetylating iNAMPT

SIRT1 enzymatic activity is effectively inhibited by nicotinamide in culture conditions (Bitterman et al., 2002). Therefore, we suspected that SIRT1 might regulate eNAMPT secretion in adipose tissue. To address this possibility, we first examined whole-body *Sirt1* knockout (*Sirt1*$^{-/-}$) mice on an FVB background. Different from other *Sirt1*$^{-/-}$ mouse lines on the B6 or 129 backgrounds, these FVB *Sirt1*$^{-/-}$ mice do not die postnatally and can grow into adulthood (Satoh et al., 2010). In *Sirt1*$^{+/+}$ mice, plasma eNAMPT levels showed moderate but significant increases in response to 48-hr fasting (Figure 2A). However, these increases were completely abrogated in *Sirt1*$^{-/-}$ mice (Figure 2A). Intriguingly, iNAMPT significantly accumulated in the WAT of *Sirt1*$^{-/-}$ mice compared to *Sirt1*$^{+/+}$ mice, whereas the iNAMPT protein levels did not differ in the liver between *Sirt1*$^{+/+}$ and *Sirt1*$^{-/-}$ mice (Figure 2B). Given that *Nampt* mRNA levels were indistinguishable in WAT between *Sirt1*$^{+/+}$ and *Sirt1*$^{-/-}$ mice (Figure 2C), this abnormal accumulation of iNAMPT in *Sirt1*$^{-/-}$ WAT is likely associated with a defect in eNAMPT secretion in *Sirt1*$^{-/-}$ mice. To further demonstrate the importance of adipose SIRT1 for the control of eNAMPT secretion, we generated adipose tissue-specific *Sirt1* knockout (*AT-Sirt1*$^{-/-}$) mice. *AT-Sirt1*$^{-/-}$ mice showed a similar phenotype to the whole-body *Sirt1*$^{-/-}$ mice (Figure 2D). Indeed, *AT-Sirt1*$^{-/-}$ mice completely failed to increase plasma eNAMPT in response to 48-hr fasting, confirming the physiological relevance of this SIRT1-mediated eNAMPT secretion from adipose tissue, particularly in response to fasting.

To further examine the role of SIRT1 in eNAMPT secretion, we overexpressed *Sirt1* or *Gfp* in differentiated HIB-1B adipocytes by adenoviral transduction and quantified eNAMPT secretion. Overexpression of SIRT1 enhanced eNAMPT secretion 2.3-fold compared to GFP controls in differentiated HIB-1B cells (Figure 3A). We further confirmed this result by introducing both NAMPT and SIRT1 into HEK293 cells, which shows negligible basal expression of both proteins. Again, overexpression of SIRT1 enhanced eNAMPT secretion, and the enhancement was much more robust in the HEK293 cells (~11-fold) compared to that in the differentiated HIB-1B cells (Figure 3B). We also assessed the acetylation status of iNAMPT in this condition. Acetylated iNAMPT was detected only in the presence of TSA and nicotinamide, and iNAMPT acetylation levels significantly decreased by SIRT1 overexpression (Figure 3C). These results, in combination with the results from *Sirt1*$^{-/-}$ and *AT-Sirt1*$^{-/-}$ mice, suggest that SIRT1-mediated deacetylation of iNAMPT predisposes the protein to secretion from differentiated adipocytes.

Because SIRT1 typically interacts directly with its deacetylation targets, we also examined whether SIRT1 and iNAMPT physically interact in differentiated adipocytes. Indeed, SIRT1 and iNAMPT did interact in differentiated HIB-1B adipocytes (Figure 3D), and this interaction appeared to be enhanced by low glucose (Figure 3D, right two lanes). Although SIRT1 is usually considered to be a nuclear sirtuin, we found that a considerable amount of SIRT1 was localized in the cytoplasm of differentiated HIB-1B and 3T3-L1 cells (Figures 3E and S1). iNAMPT was primarily localized in the cytoplasm of these adipocytes (Figures 3E and S1). Therefore, these results suggest that SIRT1 physically interacts with and deacetylates iNAMPT in the cytoplasm of differentiated adipocytes, promoting the secretion of eNAMPT.

Deacetylation of lysine 53 on iNAMPT enhances eNAMPT secretion

We next attempted to determine which acetylated residues of iNAMPT are important for the regulation of eNAMPT secretion. We established HEK293 and differentiated HIB-1B cells expressing C-terminally FLAG-tagged iNAMPT, and then FLAG-tagged iNAMPT and eNAMPT proteins were purified from those cell extracts and culture supernatants, respectively. These purified NAMPT proteins, as well as the bacterially produced recombinant NAMPT protein, were subjected to a mass spectrometric analysis of protein modification. Five lysines, K53, K79, K107, K331, and K369, were found to be acetylated on iNAMPT, whereas only K369 was acetylated on eNAMPT (Figures 4A and S2). Surprisingly, four out of the five lysines were also acetylated on bacterially produced recombinant NAMPT, although it had K339 acetylation instead of K107 (Figure 4A). This implies that regulation of NAMPT acetylation might be conserved from bacteria to mammals. Among these acetylated lysines, the location of K53 on the crystal structure of iNAMPT is particularly interesting. NAMPT is a dimeric type II phosphoribosyltrasferase, and K53, which protrudes from each monomer, is aligned along the “cleft” of the dimer and very close to the catalytic sites (Figure 4B) (Khan et al., 2006; Wang et al., 2006). Contrarily, K79 is located at the opposite side of the dimer to K53 (Figure 4B). Other acetylated lysines are located on surrounding α-helices of the dimer. We introduced the deacetylation-mimicking K-to-R mutation into K53 and/or K79 and examined the acetylation levels of each mutant iNAMPT in response to SIRT1. Whereas the wild-type and

K79R mutant iNAMPT proteins showed SIRT1-dependent deacetylation, the K53R and K53/79R mutants displayed reduced acetylation levels and did not show further reduction in acetylation levels by SIRT1 (Figure 4C), suggesting that K53 is the SIRT1-dependent acetylation site on iNAMPT. We also assessed the enzymatic activity and the secretion of this K53R mutant, as well as another mutant K53A, compared to the wild-type NAMPT in differentiated HIB-1B adipocytes. The enzymatic activity of both K53R and K53A mutants did not differ from that of the wild-type iNAMPT (Figure 4D). However, the secretion of these mutant proteins was 2.5–3-fold higher than that of the wild-type protein (Figure 4E), strongly suggesting the importance of this particular lysine and its deacetylation for the regulation of eNAMPT secretion. Conversely, introduction of the acetylation-mimicking K-to-Q mutation into K53 significantly decreases the enzymatic activity and the secretion of the protein (Figures 4F and 4G), suggesting that acetylation of lysine 53 suppresses NAMPT enzymatic activity and secretion. Taken together, these results demonstrate that eNAMPT secretion is regulated by SIRT1 through deacetylation of lysine 53 in differentiated adipocytes.

Adipose tissue-specific *Nampt* knockout mice exhibit reduced plasma eNAMPT levels and defects in NAD^+ biosynthesis not only in adipose tissue but also in the hypothalamus

Given that the secretion and enzymatic activity of eNAMPT are highly regulated by SIRT1-dependent deacetylation in differentiated adipocytes, we suspected that eNAMPT secreted by adipose tissue has a functional role as an extracellular NAD^+ biosynthetic enzyme. To address this hypothesis, we generated adipose tissue-specific *Nampt* knockout (ANKO) mice by crossing floxed *Nampt* (*Nampt*$^{flox/flox}$) mice (Rongvaux et al., 2008) and adiponectin-Cre driver mice (Eguchi et al., 2011). ANKO mice were born following the Mendelian ratio and looked overtly normal. As expected, ANKO mice showed the complete lack of iNAMPT expression in visceral WAT and BAT, although trace amounts of iNAMPT remained in subcutaneous WAT (Figure 5A). Consistent with the lack of iNAMPT, NAD^+ levels were dramatically reduced to 7–28% of the control *Nampt*$^{flox/flox}$ mice in ANKO WAT and BAT (Figure 5B), demonstrating that NAMPT functions as a major NAD^+ biosynthetic enzyme in adipose tissue. This dramatic reduction in NAD^+ levels did not seem to affect the gross structure of white adipose tissue under an *ad libitum*-fed condition. Mean white adipocyte diameter, body weight, and fat mass in ANKO mice were not significantly different from those in the control *Nampt*$^{flox/flox}$ mice (Figures S3A–C). We found that plasma eNAMPT levels significantly decreased by 30–40% in both fed and fasted conditions in ANKO females, compared to those in control *Nampt*$^{flox/flox}$ mice (Figure 5C), demonstrating that adipose tissue significantly contributes to the production of circulating eNAMPT in female mice. Contrarily, ANKO male mice did not show any detectable decreases in plasma eNAMPT levels (Figure S3E). Surprisingly, while other tissues such as the liver and skeletal muscle did not show any change in NAD^+ levels (Figure 5B), the hypothalamus, but not the hippocampus, showed significant decreases in NAD^+ levels in ANKO mice compared to controls (Figure 5D). mRNA expression levels of *Nampt* and other NAD^+ biosynthetic enzymes showed no decrease in ANKO hypothalami (Figure S3D), indicating that the reduction in NAD^+ levels detected in ANKO hypothalami was not likely due to intrinsic defects in their NAD^+ biosynthetic machineries. Consistently, mRNA expression of *Ox2r*, a SIRT1 target gene in the hypothalamus (Satoh et al., 2010; Satoh et al., 2013), was also

significantly decreased in the hypothalami of ANKO females, but not in their hippocampi (Figure 5E), indicating that NAD^+-dependent SIRT1 activity is lower in female ANKO hypothalami. Consistent with their plasma eNAMPT levels, ANKO males did not show any changes in hypothalamic NAD^+ levels (Figure S3F). These results suggest that adipose NAMPT significantly contributes to plasma eNAMPT and is important to maintain normal NAD^+ levels not only in adipose tissue but also in the hypothalamus. Because the results from *AT-Sirt1*$^{+/+}$ and *AT-Sirt1*$^{-/-}$ mice indicate that the SIRT1-mediated secretion of eNAMPT from adipose tissue is more important in response to fasting, we examined whether *AT-Sirt1*$^{-/-}$ mice show any defect in maintaining hypothalamic NAD^+ levels during fasting, compared to their *ad libitum*-fed condition. We found that hypothalamic NAD^+ levels decreased by 20% in response to fasting in control *AT-Sirt1*$^{+/+}$ mice, whereas *AT-Sirt1*$^{-/-}$ mice exhibited further decreases (40%) in hypothalamic NAD^+ levels in response to fasting (Figure S3G), supporting the physiological role of eNAMPT secretion by adipose tissue in maintaining hypothalamic NAD^+ levels.

Physical activity is reciprocally altered in loss- and gain-of-function mouse models of adipose NAMPT

In the hypothalamus, SIRT1 regulates *Ox2r* expression, and this SIRT1-mediated signaling in the hypothalamus is critical to regulate physical activity of mice during the dark time and in response to fasting (Satoh et al., 2010; Satoh et al., 2013; Satoh and Imai, 2014). Given that levels of NAD^+ and *Ox2r* expression were significantly reduced in female ANKO hypothalami, we examined their physical activity during the dark time. Interestingly, we found that female ANKO mice showed significantly reduced physical activity during the dark time (Figure 6A), consistent with reduced hypothalamic NAD^+ and *Ox2r* levels, all suggesting the impairment of SIRT1 activity in the hypothalamus. Because we have previously demonstrated that systemic administration of NMN can enhance NAD^+ biosynthesis and activate SIRT1 activity in multiple tissues (Ramsey et al., 2008; Revollo et al., 2007; Yoshino et al., 2011), we next asked whether NMN administration could rescue the observed hypothalamic functional defect in ANKO females. With the dose of NMN that our and other groups have previously used (500 mg/kg body weight) (Gomes et al., 2013; Ramsey et al., 2008; Revollo et al., 2007; Yoshino et al., 2011), we confirmed that each hypothalamic nucleus showed 1.5–3.5-fold increases in NAD^+, with a nicely grading distribution of NAD^+ from the median eminence (Elmquist et al., 1999; Rodriguez et al., 2010) towards the furthest nucleus (Figure S4A). We then injected NMN into ANKO females at 5 pm, one hour before lights were turned off. Remarkably, NMN-treated ANKO females showed significantly higher physical activity compared to PBS-injected ANKO females for the first half of the 12-hr dark time (Figure 6B). Because the enhancement of NAD^+ biosynthesis by one NMN injection lasts for ~ 6 hrs in the brain (Stein and Imai, 2014), this result provides support to our notion that the hypothalamus of ANKO females have defects in NAD^+ biosynthesis and its function. Because adipose tissue-dependent eNAMPT secretion is enhanced in response to fasting, we also examined the physical activity levels of ANKO mice after 48-hr fasting. Their physical activity levels in response to fasting were significantly reduced compared to those of control mice (Figure 6C). Contrarily, adipose tissue-specific *Nampt* knockin (ANKI) mice, which showed 2.2–2.5-fold increases in plasma eNAMPT levels under fasting in both males and females (Figure S4B),

exhibited increases in physical activity, compared to control mice, in response to fasting (Figure 6D). Consistent with this phenotype, NAD^+ levels were significantly enhanced in ANKI hypothalami, but not in ANKI hippocampi, compared to those in controls (Figure 6E). *Ox2r* expression levels, which reflects hypothalamic SIRT1 activity, were also enhanced in ANKI hypothalami (Figure 6F). Therefore, these results provide significant support to our notion that eNAMPT plays an important role in maintaining normal hypothalamic NAD^+ levels, SIRT1 activity, and physical activity, particularly in response to fasting.

A NAMPT-neutralizing antibody reduces hypothalamic NAD^+ levels *in vivo*, whereas eNAMPT enhances hypothalamic NAD^+ biosynthesis, SIRT1 activity, and neural activity *ex vivo*

To further assess whether the NAD^+ decrease observed in the ANKO hypothalamus is the direct outcome of the decrease in eNAMPT-mediated NAD^+ production, we systemically injected a NAMPT-neutralizing polyclonal antibody and control rabbit IgG into wild-type B6 male mice. This particular polyclonal antibody was able to suppress NAMPT enzymatic activity by 90% for recombinant NAMPT *in vitro* and by 40% for eNAMPT in plasma (Figure S5). Interestingly, the injection of the NAMPT-neutralizing antibody moderately but significantly reduced NAD^+ levels in the hypothalamus, but not in the hippocampus (Figure 7A), confirming the direct effect of eNAMPT on hypothalamic NAD^+ levels. To further confirm the biological relevance of eNAMPT in the regulation of hypothalamic NAD^+ levels, we established an *ex vivo* assay using hypothalamic explants. Using this assay, we examined the direct effect of eNAMPT-containing conditioned media on NAD^+ levels and neural activation measured by *cFos* expression in hypothalamic explants. Interestingly, eNAMPT-containing conditioned media were able to significantly increase NAD^+ levels and *cFos* expression in hypothalamic explants, compared to control conditioned media (Figure 7B). The extent of *cFos* activation by eNAMPT-containing conditioned media was similar to that by ghrelin, an orexigenic gut hormone known to stimulate hypothalamic neurons in rodents (Kobelt et al., 2008). Consistently, the addition of the purified eNAMPT protein to culture media was also able to significantly increase NAD^+, *cFos*, and *Ox2r* levels in hypothalamic explants (Figure 7C). These results provide further support to our notion that eNAMPT is capable of directly promoting hypothalamic NAD^+ biosynthesis, SIRT1 activity, and neural activation. Taken together, our findings indicate that NAD^+/SIRT1-mediated eNAMPT secretion from adipose tissue plays a critical role in the regulation of hypothalamic NAD^+ biosynthesis and function.

DISCUSSION

Our present study has demonstrated that the secretion and enzymatic activity of eNAMPT are regulated by SIRT1-dependent deacetylation in adipocytes. Indeed, this highly regulated process appears to be important particularly in adipose tissue in response to changes in nutritional availability. Interestingly, SIRT1 and NAMPT comprise a novel transcriptional-enzymatic feedback loop that produces a circadian oscillation of NAD^+ in peripheral tissues (Nakahata et al., 2009; Ramsey et al., 2009). Our present study has revealed that SIRT1 and NAMPT comprise another NAD^+-regulatory feedback loop through the regulation of

eNAMPT secretion from adipose tissue. In this new mechanism, SIRT1-dependent deacetylation of iNAMPT at lysine 53 predisposes the protein to secretion. The deacetylation event seems to occur in the cytoplasm of differentiated adipocytes, and approximately 0.5% of iNAMPT per hour is estimated to be secreted as eNAMPT in differentiated HIB-1B adipocytes (data not shown), suggesting that a very specific fraction of iNAMPT is destined to enter this SIRT1-dependent secretory machinery. The experiments with K-to-R and K-to-Q mutants of lysine 53 demonstrate that the acetylation status of lysine 53 is critical to determine the fate of iNAMPT. Because the K53A mutation also significantly increases eNAMPT secretion, lysine 53 *per se* appears to play an important role in determining the fate of iNAMPT, possibly providing a docking site to an unidentified factor that might interact with acetylated lysine 53 of iNAMPT and prevent it from secretion (Figure 7D).

Acetylation is also important to regulate the enzymatic activity of NAMPT. We identified five acetylation sites on iNAMPT, and four out of these five sites are found to be deacetylated on eNAMPT. The enzymatic activity of iNAMPT is 2–4-fold lower than that of eNAMPT (Revollo et al., 2007), and the K53Q mutant can recapitulate this acetylation-dependent reduction in the enzymatic activity. Lysine 53 is distinguished from other lysine residues because of its location at the “cleft” which contains the catalytic sites, although other lysines might have other functions in different biological contexts. These results indicate that acetylation/deacetylation might induce a conformational change in NAMPT structure and regulate its enzymatic activity. It will be of great interest to examine what effects the acetylation of lysine 53 makes on the structure of the catalytic sites and dimer formation of NAMPT. Because NAD^+ drives SIRT1 activity in a circadian oscillatory manner (Nakahata et al., 2009; Ramsey et al., 2009), it is also likely that deacetylation and secretion of eNAMPT follow circadian oscillation. Indeed, plasma eNAMPT levels appear to show diurnal oscillation in mice, although it is still unclear whether this oscillation is produced by an intrinsic clock mechanism (unpublished observation). Therefore, our findings provide an interesting possibility that the intimate interplay between SIRT1 and NAMPT contributes to multi-layered feedback loops regulating the dynamics of NAD^+ biosynthesis within and between tissues and organs.

Why does adipose tissue secrete a key NAD^+ biosynthetic enzyme to blood circulation? We have obtained important clues to this question from adipose tissue-specific *Nampt* knockout (ANKO) mice. Interestingly, ANKO females, but not males, show significant decreases in plasma eNAMPT levels. A surprising finding is that the adipose tissue-specific deficiency of NAMPT causes significant reduction in NAD^+ levels not only in WAT and BAT, but also in some remote tissues, specifically the hypothalamus. Because the hypothalami of ANKO females do not have any obvious defects in their endogenous NAD^+ biosynthetic machineries, the observed reduction in NAD^+ levels is likely attributed to the NAMPT deficiency in adipose tissue. Furthermore, the defect appears to be specific at least to the hypothalamus because other tissues and organs, including the liver, skeletal muscle, and the hippocampus, do not show any reduction in NAD^+ levels. Consistent with reduced NAD^+ levels, ANKO female mice also show significant reduction in the mRNA expression levels of *Ox2r*, a critical hypothalamic SIRT1 target gene, and their physical activity during the

dark time. This hypothalamic functional defect can be ameliorated, at least partially, by a single injection of NMN. Additionally, the results from the systemic injection of a NAMPT-neutralizing antibody and *ex vivo* hypothalamic explant assays provide further support for our conclusion that eNAMPT regulates hypothalamic NAD^+ production and function. This role of eNAMPT in maintaining normal hypothalamic NAD^+ levels appears to be more important in fasting because *AT-Sirt1*$^{-/-}$ mice had a defect in fasting-induced plasma eNAMPT increase and also showed further decreases in hypothalamic NAD^+ levels, compared to controls, in response to fasting. Consistent with this notion, loss- and gain-of-function mouse models of adipose NAMPT, namely, ANKO and ANKI mice, reciprocally change their plasma eNAMPT levels and physical activity, as well as their hypothalamic NAD^+ and *Ox2r* expression levels, in response to fasting.

Although how exactly eNAMPT regulates hypothalamic NAD^+ levels and neuronal activity is still under investigation, it is conceivable that eNAMPT secreted from adipose tissue plays a critical role in supplying NMN to the hypothalamus. The hypothalamus has a low level of NAMPT expression, implying that this tissue might require the extracellular supply of NMN, possibly through the median eminence (Elmquist et al., 1999; Rodriguez et al., 2010), for the maintenance of its optimal NAD^+ biosynthesis. Our finding that adipose tissue actively regulates the secretion and enzymatic activity of eNAMPT in an NAD^+/SIRT1-dependent manner provides strong support to the idea that adipose tissue functions as a critical determinant for the spatial and temporal coordination of NAD^+ biosynthesis throughout the body. This systemic coordination of NAD^+ biosynthesis might play an important role in orchestrating metabolic responses in multiple tissues and maintaining metabolic homeostasis against nutritional and environmental perturbations. In this highly coordinated systemic network, adipose tissue modulates the functions of remote tissues, such as the hypothalamus, through the NAD^+/SIRT1-dependent regulation of eNAMPT secretion. This model also predicts that having an optimal amount of adipose tissue might be beneficial to maximize the robustness of the physiological system through the regulation of systemic NAD^+ biosynthesis. Further investigation on the system dynamics of this novel network will provide insight into the role of adipose tissue as a critical modulator for the regulation of systemic NAD^+ biosynthesis.

Experimental Procedures

Detection of intracellular NAMPT and SIRT1 in tissues, and of extracellular NAMPT in plasma

Mice fed *ad libitum* or fasted for 48 hr were euthanized by carbon dioxide asphyxiation. Organs were immediately collected, homogenized in 1X Laemmli's sample buffer using a Polytron (Kinematica, Switzerland), and boiled for 5 minutes. Samples were then centrifuged at 16000g, and protein concentrations were measured by the Bradford assay (Bio-Rad, CA). Plasma samples from mice fed *ad libitum* or fasted for 48 hr were collected by centrifuging blood at 3200g for 5 minutes at 4°C and immediately boiled for 5 minutes in 1X Laemmli's sample buffer. Tissue extracts and plasma samples were analyzed by Western blotting with anti-NAMPT (Bethyl Laboratories, TX) or anti-SIRT1 (Sigma, MO)

antibodies. For plasma samples, equal loading was confirmed by Ponceau S staining of membranes.

Detection of acetylated NAMPT in adipose tissue and differentiated HIB-1B cells

WAT and BAT collected from wild-type FVB mice were homogenized in 1X RIPA buffer [50 mM Tris-HCl, pH 8.0, 150 mM NaCl, 1% Igepal CA630, 0.5% Sodium deoxycholate, 0.1% SDS, 1 mM EDTA, 1 mM NaF, 10 μM Trichostatin A, 10 mM nicotinamide, 0.5 mM DTT, protease inhibitor cocktail (Roche, Germany)]. Tissue extracts were immunoprecipitated with anti-acetyl lysine antibody-conjugated beads (ImmuneChem, Canada) overnight. Immunoprecipitates were eluted with 1X Laemmli's sample buffer, boiled for 5 minutes, and analyzed by Western blotting with an anti-NAMPT antibody (OMNI379, Enzo Life Science, NY). Fully differentiated HIB-1B cells were homogenized in NAMPT-IP buffer [PBS (pH 7.4), 0.5% NP-40, 1 mM EDTA, 1 mM NaF, 10 μM Trichostatin A, 10 mM nicotinamide, 0.5 mM DTT, protease inhibitor cocktail (Roche, Germany)], and cell extracts were immunoprecipitated with an anti-acetyl lysine antibody (Cell signaling, MA) or an anti-NAMPT antibody (Bethyl Laboratories) and protein A agarose (Sigma, MO). NAMPT was detected by Western blotting with the same anti-NAMPT antibody and light-chain anti-rabbit IgG (Jackson ImmunoResearch).

Generation of HIB-1B cells stably expressing wild type or mutant NAMPT-FLAG

A C-terminally FLAG-tagged NAMPT (NAMPT-FLAG) was created and cloned into the mammalian expression vector pCXN2 as described previously (Revollo et al., 2007). Each lysine mutant NAMPT-FLAG was generated using the QuikChange II Site-Directed Mutagenesis Kit (Stratagene, CA) according to the manufacturer's protocol. To create HIB-1B cells expressing NAMPT-FLAG or mutant NAMPT-FLAG, HIB-1B pre-adipocytes were transfected (Superfect, QIAGEN, CA) with pCXN2-NAMPT-FLAG or pCXN2-mutant NAMPT-FLAG. Transfected HIB-1B cells were selected by incubating with 500 μg/ml of G418 (Invitrogen, CA) for 2 weeks. Before the secretion assay and the enzymatic reactions, HIB-1B cells were fully differentiated as described above.

eNAMPT secretion assay

3T3-L1 or HIB-1B cells were differentiated as described above. To detect endogenous iNAMPT or eNAMPT, cell extracts or culture supernatant were collected, respectively, immunoprecipitated as described previously (Revollo et al., 2007), and analyzed by Western blotting with an anti-NAMPT polyclonal antibody (Bethyl Laboratories, TX). HEK293 cells transfected with NAMPT-FLAG and HIB-1B cells stably expressing NAMPT-FLAG were processed in the same way, except that anti-FLAG beads (M2, Sigma, MO) were used for immunoprecipitation. eNAMPT secretion levels were calculated as (eNAMPT levels/iNAMPT levels)/the amount of total protein in cell lysates or eNAMPT levels/(iNAMPT levels/ACTIN levels)/the amount of total protein in cell lysates by quantifying Western blotting results.

Enzymatic reactions

NAMPT enzymatic reactions were conducted as previously described (Revollo et al., 2007). For immunoprecipitation of iNAMPT-FLAG, whole cell extracts were prepared with NAMPT-IP buffer and mixed with anti-FLAG-M2 conjugated beads (Sigma, MO) for 2–3 hours at 4°C. For immunoprecipitation of eNAMPT-FLAG, HIB-1B culture supernatants were collected after incubating differentiated HIB-1B cells overnight with DMEM without fetal bovine serum but supplemented with 5 mg/ml insulin and 1 nM triiodothyronine, centrifuged at 3000 rpm for 2 min at 4°C, concentrated 8 to 10 fold with Amicon Ultra-15 columns (Milipore, MA), and mixed with anti-FLAG beads for 2–3 hr at 4°C. Immunoprecipitates were washed twice with IP-buffer and twice with PBS.

Immunoprecipitates on anti-FLAG beads were incubated in enzymatic reaction buffer [50 mM Tris-HCl, pH 8.5, 100 mM NaCl, 0.25 mM nicotinamide, 10 mM $MgSO_4$, 1.5% ethanol, 0.5 mM phosphoribosyl phyrophosphate (PRPP), 2 mM ATP] for 55 min at 37°C. After this reaction, mouse recombinant NMNAT and yeast alcohol dehydrogenase were added at a final concentration of 10 mg/ml each, and the mixture was incubated for 5 min at 37°C. Supernatants were collected by spinning down anti-FLAG beads, and auto-fluorescence of NADH was measured in a PerkinElmer LS 50B fluorometer (340 nm excitation, 460 nm emission). NADH auto-fluorescence values were converted to the amount of NMN using a standard curve drawn with known amounts of NMN. Immunoprecipitates bound on anti-FLAG beads were extracted with 1X Laemmli's buffer, boiled for 5 min, and analyzed by Western blotting with an anti-NAMPT antibody. The amounts of NAMPT used for enzymatic reactions were quantitated compared to the standards of mouse recombinant NAMPT. K_{cat} values were calculated based on the molar amount of NMN generated per molar amount of immunoprecipitated NAMPT-FLAG proteins per unit time.

Generation of *AT-Sirt1*$^{-/-}$, ANKO and ANKI mice and measurement of their physical activity levels

Sirt1$^{flox/flox}$ mice were generated by flanking the exon 3 of the *Sirt1* gene by loxP sites (Takikawa et al, submitted). *Nampt*$^{flox/flox}$ mice, Cre-inducible STOP-*Nampt* mice, and Adiponectin-Cre mice were generously provided by Dr. Oberdan Leo at Université de Léige, Belgium (Rongvaux et al., 2008), Dr. Joseph Baur at University of Pennsylvania (Frederick et al., 2014), and Dr. Evan Rosen at Beth Israel Deaconess Medical Center (Eguchi et al., 2011), respectively. All lines were backcrossed to the C57BL/6J background. Adiponectin-Cre mice were mated with *Sirt1*$^{flox/flox}$, *Nampt*$^{flox/flox}$, or STOP-*Nampt* mice, and cohorts were established by mating F1 *Sirt1*$^{flox/+}$;Cre or *Nampt*$^{flox/+}$;Cre to *Sirt1*$^{flox/flox}$ or *Nampt*$^{flox/flox}$ mice, respectively. *Sirt1*$^{flox/flox}$;Cre and *Nampt*$^{flox/flox}$;Cre were considered as *AT-Sirt1*$^{-/-}$ and ANKO mice, respectively. *Sirt1*$^{flox/flox}$;+ and *Nampt*$^{flox/flox}$;+ were used as controls. For ANKI mice, Cre-induced heterozygous mice were used, and Cre-minus littermates were used as controls. When necessary, synchronized females were used. For synchronization of female estrus cycle, female mice were exposed to bedding from male cages for 3 days. Wheel-running activity of mice was recorded and evaluated as described previously (Satoh et al., 2010). Physical activity after 48-hr fasting was measured by counting the numbers of quadrants crossed during 10 min in recorded videos of each cage

containing 5 mice (Satoh et al., 2010). All animal procedures were approved by the Washington University Animal Studies Committee and were in accordance with NIH guidelines.

In vivo eNAMPT neutralization

20 μg of anti-NAMPT rabbit antibody (Bethyl Laboratory, TX) or control rabbit IgG (Sigma, MO) were diluted in 100 μl PBS. 100 μl of the solution were injected to 3–4 week-old age-matched male mice intravenously via tail vein. One hour post injection, injected mice were sacrificed and hypothalamus was collected. Hypothalamic samples were stored frozen until analysis.

Ex vivo hypothalamic explant culture

Hypothalami were collected from 1–12 week-old mice and cut into hemihypothalami along the sagittal plane. Biologically-matched hemihypothalami were incubated with either eNAMPT-containing or control conditioned media for 1 hr at 37°C. In separate experiments, hemihypothalami were incubated with serum-free media (50 μl) supplemented with 1μg of either the eNAMPT protein purified from HEK293 culture supernatants (Adipogen) or BSA for 3 hr at 37°C. Hypothalamic samples were stored frozen until analysis. Quantitative real-time RT-PCR was conducted with the TaqMan Fast Universal PCR Master mix and TaqMan primers for *cFos* and *Gapdh* in the GeneAmp 7500 fast sequence detection system (Applied Biosystems). Relative gene expression levels were calculated by normalizing to *Gapdh* levels and then to the mean of control hypothalamic explants.

Statistical Analysis

Differences between two groups were assessed using the Student's *t* test. Comparisons among several groups were performed using one-way ANOVA with the Fisher's LSD *posthoc* test. p values equal to or less than 0.05 were considered statistically significant. All values were presented as mean ± standard error of the mean (SEM).

Supplementary Material

Refer to Web version on PubMed Central for supplementary material.

Acknowledgments

We thank James Skinner for his advice on detecting iNAMPT acetylation in adipose tissue; Ross Tomaino, Basil Hubbard, and David Sinclair for mass spectrometry analysis in the Taplin Mass Spectrometry Facility at Harvard University; Akiko Satoh for the technical support on dissecting hypothalamus and hippocampus; Mia Wallace for her advice on female mouse synchronization; Terri Pietka for adipocyte size measurement in the Nutrition Obesity Research Center at Washington University School of Medicine (P30 DK56341); and Erik Herzog for providing his mouse facility to measure wheel-running activity. We also thank Thomas Baranski, Nada Abumrad, Jeffrey Milbrandt, Kelle Moley, Jean Schaffer, and members of the Imai lab for critical comments and suggestions on this manuscript. This work was supported by grants from the National Institute on Aging (AG024150, AG037457, AG047902) and the Ellison Medical Foundation to S.I. S.I. and J.Y. are also members of the Diabetes Research Center of Washington University School of Medicine (P30 DK020579). T.N. and K.T. were supported by Grants-in-Aid for Scientific Research from the Ministry of Education, Science, Sports, and Culture, Japan (26461327) and JSPS KAKENHI Grant (24689019), respectively. S.I. is a co-founder of Metro Midwest Biotech.

References

Bitterman KJ, Anderson RM, Cohen HY, Latorre-Esteves M, Sinclair DA. Inhibition of silencing and accelerated aging by nicotinamide, a putative negative regulator of yeast sir2 and human SIRT1. J Biol Chem. 2002; 277:45099–45107. [PubMed: 12297502]

Eguchi J, Wang X, Yu S, Kershaw EE, Chiu PC, Dushay J, Estall JL, Klein U, Maratos-Flier E, Rosen ED. Transcriptional control of adipose lipid handling by IRF4. Cell Metab. 2011; 13:249–259. [PubMed: 21356515]

Elmquist JK, Elias CF, Saper CB. From lesions to leptin: hypothalamic control of food intake and body weight. Neuron. 1999; 22:221–232. [PubMed: 10069329]

Frederick DW, Davis JG, Davila A Jr, Agarwal B, Michan S, Puchowicz MA, Nakamaru-Ogiso E, Baur JA. Increasing NAD Synthesis in Muscle via Nicotinamide Phosphoribosyltransferase is not Sufficient to Promote Oxidative Metabolism. J Biol Chem. 2014 Epub on Nov 19.

Fukuhara A, Matsuda M, Nishizawa M, Segawa K, Tanaka M, Kishimoto K, Matsuki Y, Murakami M, Ichisaka T, Murakami H, et al. Visfatin: a protein secreted by visceral fat that mimics the effects of insulin. Science. 2005; 307:426–430. [PubMed: 15604363]

Fukuhara A, Matsuda M, Nishizawa M, Segawa K, Tanaka M, Kishimoto K, Matsuki Y, Murakami M, Ichisaka T, Murakami H, et al. Retraction. Science. 2007; 318:565b. [PubMed: 17962537]

Garten A, Petzold S, Korner A, Imai S, Kiess W. Nampt: linking NAD biology, metabolism and cancer. Trends Endocrinol Metab. 2009; 20:130–138. [PubMed: 19109034]

Gomes AP, Price NL, Ling AJ, Moslehi JJ, Montgomery MK, Rajman L, White JP, Teodoro JS, Wrann CD, Hubbard BP, et al. Declining NAD(+) Induces a Pseudohypoxic State Disrupting Nuclear-Mitochondrial Communication during Aging. Cell. 2013; 155:1624–1638. [PubMed: 24360282]

Houtkooper RH, Canto C, Wanders RJ, Auwerx J. The secret life of NAD+: an old metabolite controlling new metabolic signaling pathways. Endocr Rev. 2010; 31:194–223. [PubMed: 20007326]

Imai S. Nicotinamide phosphoribosyltransferase (Nampt): a link between NAD biology, metabolism, and diseases. Curr Pharm Des. 2009; 15:20–28. [PubMed: 19149599]

Imai S, Guarente L. NAD^+ and sirtuins in aging and disease. Trends in cell biology. 2014; 24:464–471. [PubMed: 24786309]

Khan JA, Tao X, Tong L. Molecular basis for the inhibition of human NMPRTase, a novel target for anticancer agents. Nat Struct Mol Biol. 2006; 13:582–588. [PubMed: 16783377]

Kobelt P, Wisser AS, Stengel A, Goebel M, Inhoff T, Noetzel S, Veh RW, Bannert N, van der Voort I, Wiedenmann B, et al. Peripheral injection of ghrelin induces Fos expression in the dorsomedial hypothalamic nucleus in rats. Brain Res. 2008; 1204:77–86. [PubMed: 18329635]

Martin P, Shea R, Mulks M. Identification of a plasmid-encoded gene from *Haemophilus ducreyi* which confers NAD independence. J Bacteriol. 2001; 183:1168–1174. [PubMed: 11157928]

Miller ES, Heidelberg JF, Eisen JA, Nelson WC, Durkin AS, Ciecko A, Feldblyum TV, White O, Paulsen IT, Nierman WC, et al. Complete genome sequence of the broad-host-range vibriophage KVP40: comparative genomics of a T4-related bacteriophage. J Bacteriol. 2003; 185:5220–5233. [PubMed: 12923095]

Nakahata Y, Sahar S, Astarita G, Kaluzova M, Sassone-Corsi P. Circadian control of the NAD+ salvage pathway by CLOCK-SIRT1. Science. 2009; 324:654–657. [PubMed: 19286518]

Ramsey KM, Mills KF, Satoh A, Imai S. Age-associated loss of Sirt1-mediated enhancement of glucose-stimulated insulin secretion in β cell-specific Sirt1-overexpressing (BESTO) mice. Aging Cell. 2008; 7:78–88. [PubMed: 18005249]

Ramsey KM, Yoshino J, Brace CS, Abrassart D, Kobayashi Y, Marcheva B, Hong HK, Chong JL, Buhr ED, Lee C, et al. Circadian clock feedback cycle through NAMPT-mediated NAD^+ biosynthesis. Science. 2009; 324:651–654. [PubMed: 19299583]

Revollo JR, Grimm AA, Imai S. The NAD biosynthesis pathway mediated by nicotinamide phosphoribosyltransferase regulates Sir2 activity in mammalian cells. J Biol Chem. 2004; 279:50754–50763. [PubMed: 15381699]

Revollo JR, Körner A, Mills KF, Satoh A, Wang T, Garten A, Dasgupta B, Sasaki Y, Wolberger C, Townsend RR, et al. Nampt/PBEF/visfatin regulates insulin secretion in β cells as a systemic NAD biosynthetic enzyme. Cell Metab. 2007; 6:363–375. [PubMed: 17983582]

Rodriguez EM, Blazquez JL, Guerra M. The design of barriers in the hypothalamus allows the median eminence and the arcuate nucleus to enjoy private milieus: the former opens to the portal blood and the latter to the cerebrospinal fluid. Peptides. 2010; 31:757–776. [PubMed: 20093161]

Rongvaux A, Galli M, Denanglaire S, Van Gool F, Drèze PL, Szpirer C, Bureau F, Andris F, Leo O. Nicotinamide phosphoribosyl transferase/pre-B cell colony-enhancing factor/visfatin is required for lymphocyte development and cellular resistance to genotoxic stress. J Immunol. 2008; 181:4685–4695. [PubMed: 18802071]

Rongvaux A, Shea RJ, Mulks MH, Gigot D, Urbain J, Leo O, Andris F. Pre-B-cell colony-enhancing factor, whose expression is up-regulated in activated lymphocytes, is a nicotinamide phosphoribosyltransferase, a cytosolic enzyme involved in NAD biosynthesis. Eur J Immunol. 2002; 32:3225–3234. [PubMed: 12555668]

Samal B, Sun Y, Stearns G, Xie C, Suggs S, McNiece I. Cloning and characterization of the cDNA encoding a novel human pre-B-cell colony-enhancing factor. Mol Cell Biol. 1994; 14:1431–1437. [PubMed: 8289818]

Satoh A, Brace CS, Ben-Josef G, West T, Wozniak DF, Holtzman DM, Herzog ED, Imai S. SIRT1 promotes the central adaptive response to diet restriction through activation of the dorsomedial and lateral nuclei of the hypothalamus. J Neurosci. 2010; 30:10220–10232. [PubMed: 20668205]

Satoh A, Brace CS, Rensing N, Cliften P, Wozniak DF, Herzog ED, Yamada KA, Imai S. Sirt1 Extends Life Span and Delays Aging in Mice through the Regulation of Nk2 Homeobox 1 in the DMH and LH. Cell Metab. 2013; 18:416–430. [PubMed: 24011076]

Satoh A, Imai S. Systemic regulation of mammalian ageing and longevity by brain sirtuins. Nat Commun. 2014; 5:4211. [PubMed: 24967620]

Stein LR, Imai S. The dynamic regulation of NAD metabolism in mitochondria. Trends Endocrinol Metab. 2012; 23:420–428. [PubMed: 22819213]

Stein LR, Imai S. Specific ablation of Nampt in adult neural stem cells recapitulates their functional defects during aging. EMBO J. 2014; 33:1321–1340. [PubMed: 24811750]

Wang T, Zhang X, Bheda P, Revollo JR, Imai S, Wolberger C. Structure of Nampt/PBEF/visfatin, a mammalian NAD(+) biosynthetic enzyme. Nat Struct Mol Biol. 2006; 13:661–662. [PubMed: 16783373]

Yoshino J, Mills KF, Yoon MJ, Imai S. Nicotinamide mononucleotide, a key NAD(+) intermediate, treats the pathophysiology of diet- and age-induced diabetes in mice. Cell Metab. 2011; 14:528–536. [PubMed: 21982712]

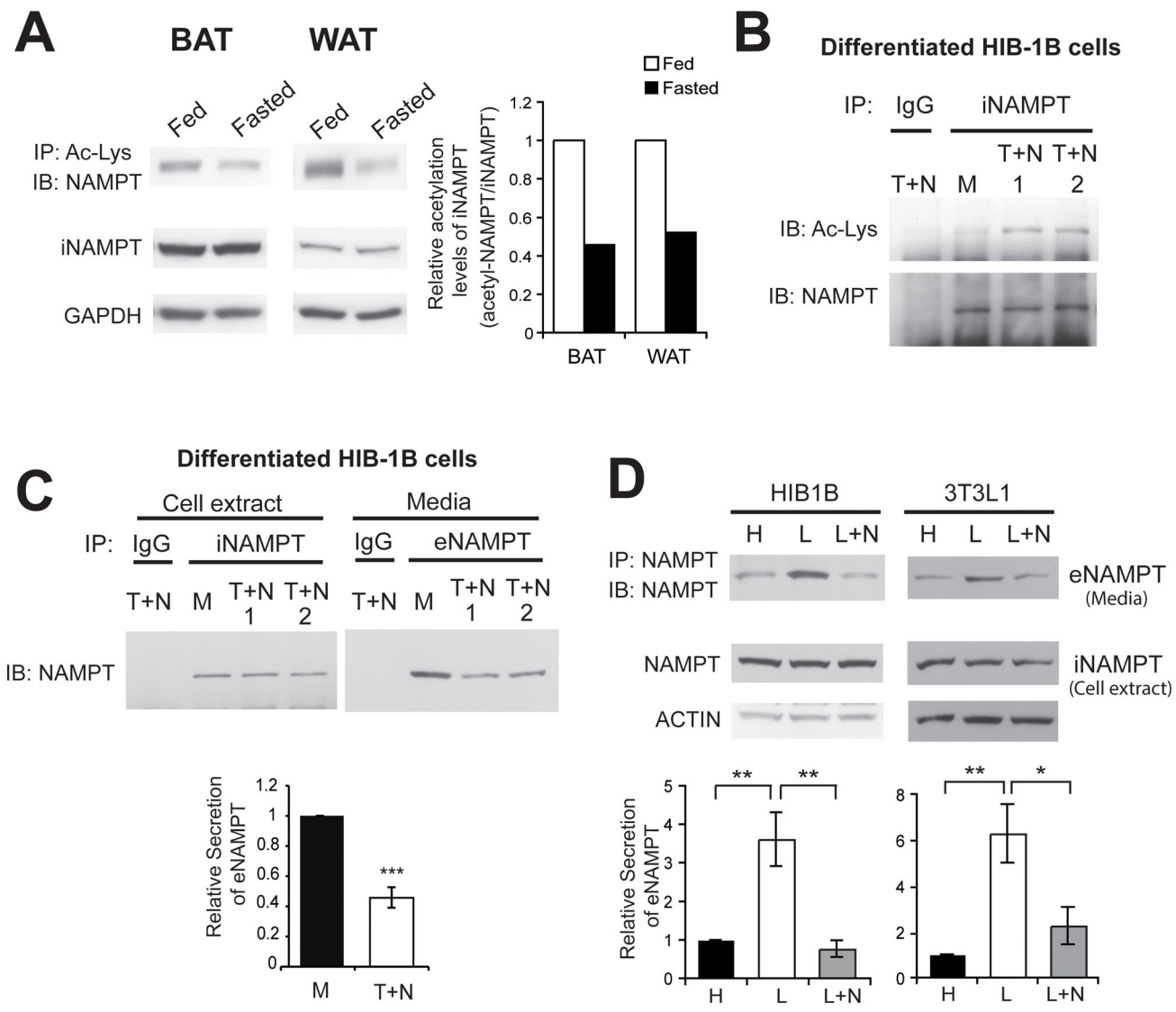

Figure 1.

iNAMPT acetylation levels decrease in response to fasting in adipose tissue and are associated with eNAMPT secretion in differentiated adipocytes. (**A**) iNAMPT acetylation levels in brown and white adipose tissues (BAT and WAT) of fed and fasted wild-type female mice at 4–5 months of age. The right panel represents average values from two independent experiments. Relative iNAMPT acetylation levels are normalized to fed values. (**B**) iNAMPT acetylation levels in differentiated HIB-1B cells. Cells were treated with 5 μM Trichostatin A (T) and 5 mM nicotinamide (N) for 3 hr. M; mock treatment. (**C**) Reduction of eNAMPT secretion after Trichostatin A (T) and nicotinamide (N) treatment in differentiated HIB-1B cells. Levels of eNAMPT secretion were calculated as described in Materials and Methods. (**D**) Enhancement of eNAMPT secretion in response to low glucose in differentiated HIB-1B cells and 3T3-L1 cells. Cells were incubated with high glucose (H, 25 mM) or low glucose (L, 5 mM) media in the presence or absence of nicotinamide (N, 5 mM) for 3 hr. Bottom panels in C and D represent average values of three independent

experiments. Each value is normalized to values from the mock (C) or the high glucose condition (D). Data were analyzed by the Student's *t* test or one-way ANOVA with Fisher's LSD *posthoc* test. All values are presented as mean ± SEM. *$p \leq 0.05$; **$p \leq 0.01$; ***$p \leq 0.001$

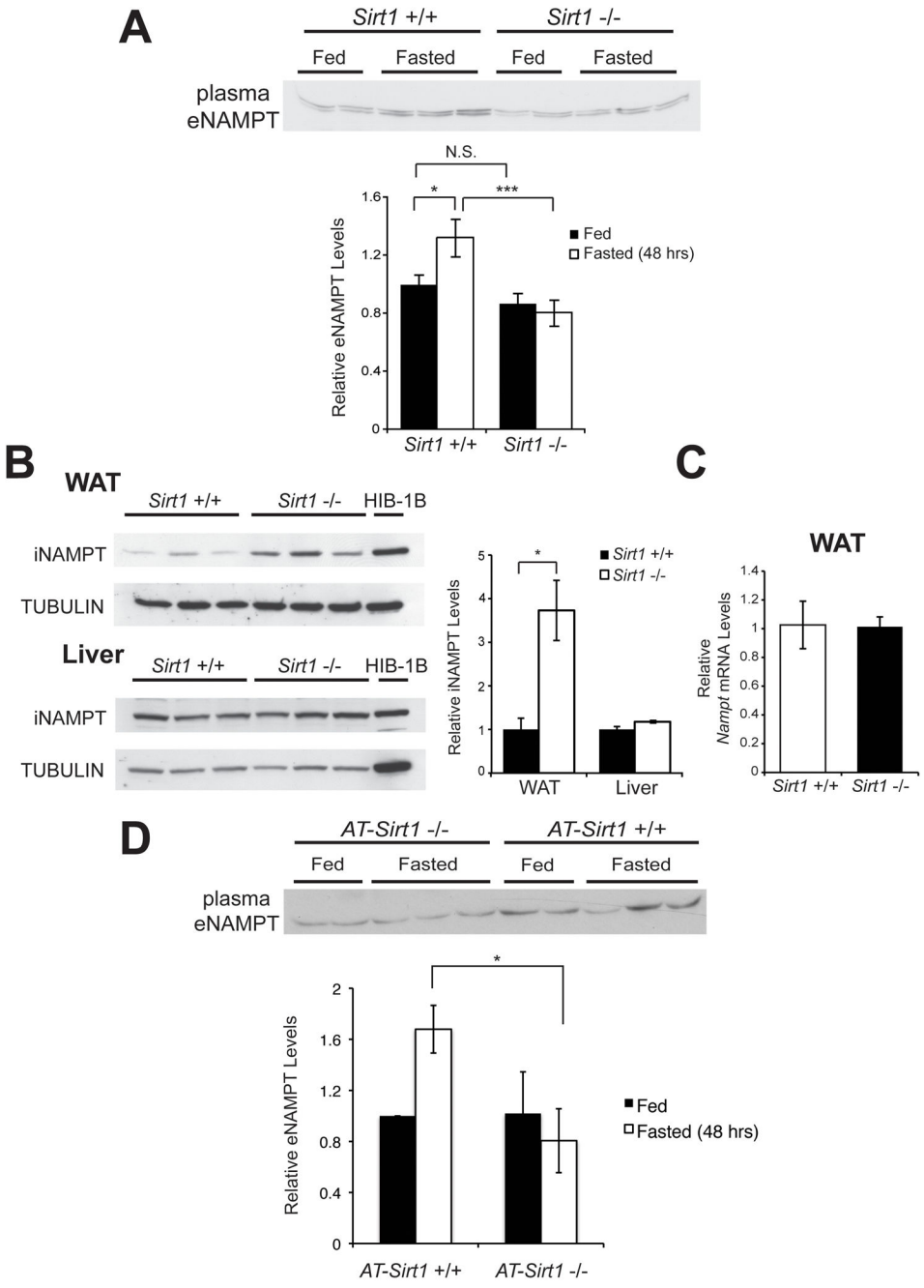

Figure 2.

Plasma eNAMPT levels increase in response to fasting in a SIRT1-dependent manner. (**A**) Plasma eNAMPT levels from fed or 48 hr-fasted *Sirt1*$^{+/+}$ and *Sirt1*$^{-/-}$ male mice at 4–5 months of age (n= 7–12). The bottom panel shows average plasma eNAMPT levels normalized to the fed *Sirt1*$^{+/+}$ level in each condition. (**B**) iNAMPT and SIRT1 protein levels in white adipose tissue (WAT) and the liver of *Sirt1*$^{+/+}$ and *Sirt1*$^{-/-}$ male mice at 3–4 months of age. iNAMPT levels are normalized to TUBULIN levels. The right panel shows average values normalized to the fed value in each tissue (n=3). (**C**) *Nampt* mRNA

expression levels in WAT of *Sirt1*$^{+/+}$ and *Sirt1*$^{-/-}$ male mice at 3–4 months of age (n= 4). (**D**) Plasma eNAMPT levels from fed or 48 hr-fasted *AT-Sirt1*$^{+/+}$ and *AT-Sirt1*$^{-/-}$ female mice at 6 months of age (n=5). Data were analyzed by the Student's *t* test or one-way ANOVA with the Fisher's LSD *post-hoc* test. All values are presented as mean ± SEM. *p ≤ 0.05; ***p ≤ 0.001.

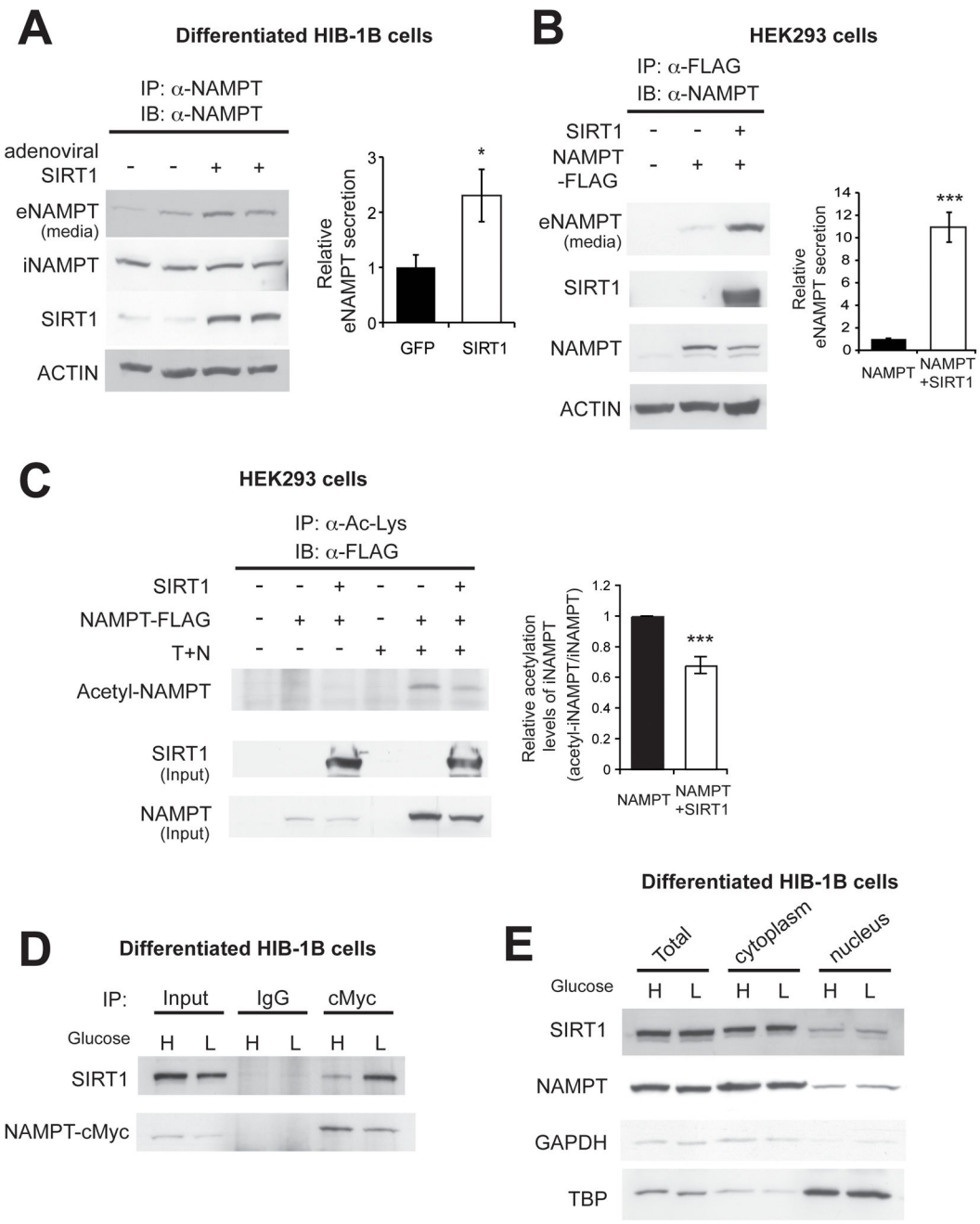

Figure 3.

SIRT1 promotes eNAMPT secretion by deacetylating iNAMPT. (**A** and **B**) SIRT1 overexpression promotes eNAMPT secretion in differentiated HIB-1B cells (**A**) and HEK293 cells (**B**). Levels of eNAMPT secretion were calculated as described in Materials and Methods. The right panels represent average values from three independent experiments. Each value is normalized to those of GFP- or NAMPT-expressing cells. (**C**) SIRT1 overexpression decreases iNAMPT acetylation levels in HEK293 cells. Cells were incubated in the absence or presence of 5 μM Trichostatin A (T) and 5 mM nicotinamide (N) overnight prior to cell lysis. Acetylated iNAMPT levels are normalized to total iNAMPT

levels. The right panel represents iNAMPT acetylation levels normalized to total iNAMPT levels in each condition (n=3). (**D**) Interaction between SIRT1 and iNAMPT in differentiated HIB-1B cells. (**E**) Subcellular localization of SIRT1 and iNAMPT in differentiated HIB-1B cells. GAPDH and TBP were examined as representative cytoplasmic and nuclear proteins, respectively. Cells were incubated with media containing high glucose (H, 25mM) or low glucose (L, 5 mM) overnight (**D**) or for 3 hr (**E**). Data were analyzed by the Student's *t* test. All values are presented as mean ± SEM. *$p \leq 0.05$; **$p \leq 0.01$; ***$p \leq 0.001$.

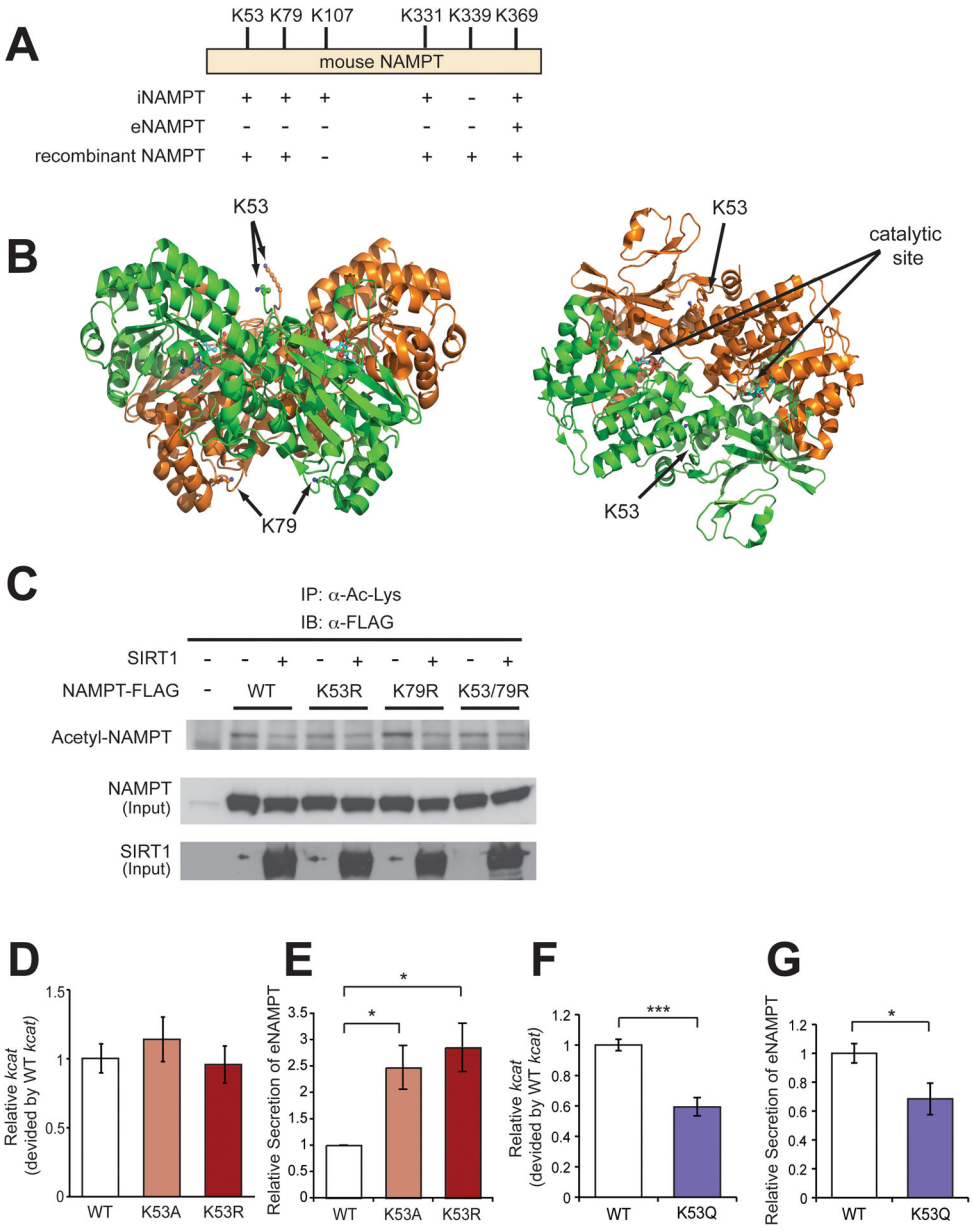

Figure 4.

Deacetylation of lysine 53 on iNAMPT enhances eNAMPT secretion and enzymatic activity. (**A**) Acetyl-lysines detected on iNAMPT and eNAMPT prepared from cell lysate of HEK293 cells and culture supernatant of differentiated HIB-1B cells, respectively. HEK293 cells overexpressing C-terminally FLAG-tagged mouse NAMPT were treated with 5 μM Trichostatin A and 5 mM nicotinamide overnight prior to cell lysis. FLAG-tagged iNAMPT and eNAMPT were immunopurified and subjected to mass spectrometric analysis. Recombinant mouse NAMPT was also prepared from bacteria. (**B**) The location of K53 and K79 on the crystal structure of dimeric NAMPT (arrows). Each monomer is shown in orange or green, and NMN molecules bound to the catalytic sites (arrows) are shown in blue. (**C**) Changes in the acetylation status of wild-type (WT) or mutant (K53R, K79R, and

K53/79R) iNAMPT by SIRT1 in HEK293 cells. Cells were treated with 5 μM Trichostatin A and 5 mM nicotinamide overnight prior to cell lysis. (**D** and **F**) The relative enzymatic activity of wild-type (WT) and mutant iNAMPT from differentiated HIB-1B cells. The enzymatic activity was determined as described in Materials and Methods. Each enzymatic activity is normalized to that of wild-type NAMPT (n=2–6). (**E** and **G**) Secretion of wild-type (WT) and mutant eNAMPT. Levels of eNAMPT secretion were calculated as described in Materials and Methods. Each value is normalized to the WT value. Each panel represents averages from three independent experiments. Data were analyzed by the Student's *t* test or one-way ANOVA with the Fisher's LSD *posthoc* test. All values are presented as mean ± SEM. *$p \leq 0.05$; ***$p \leq 0.001$.

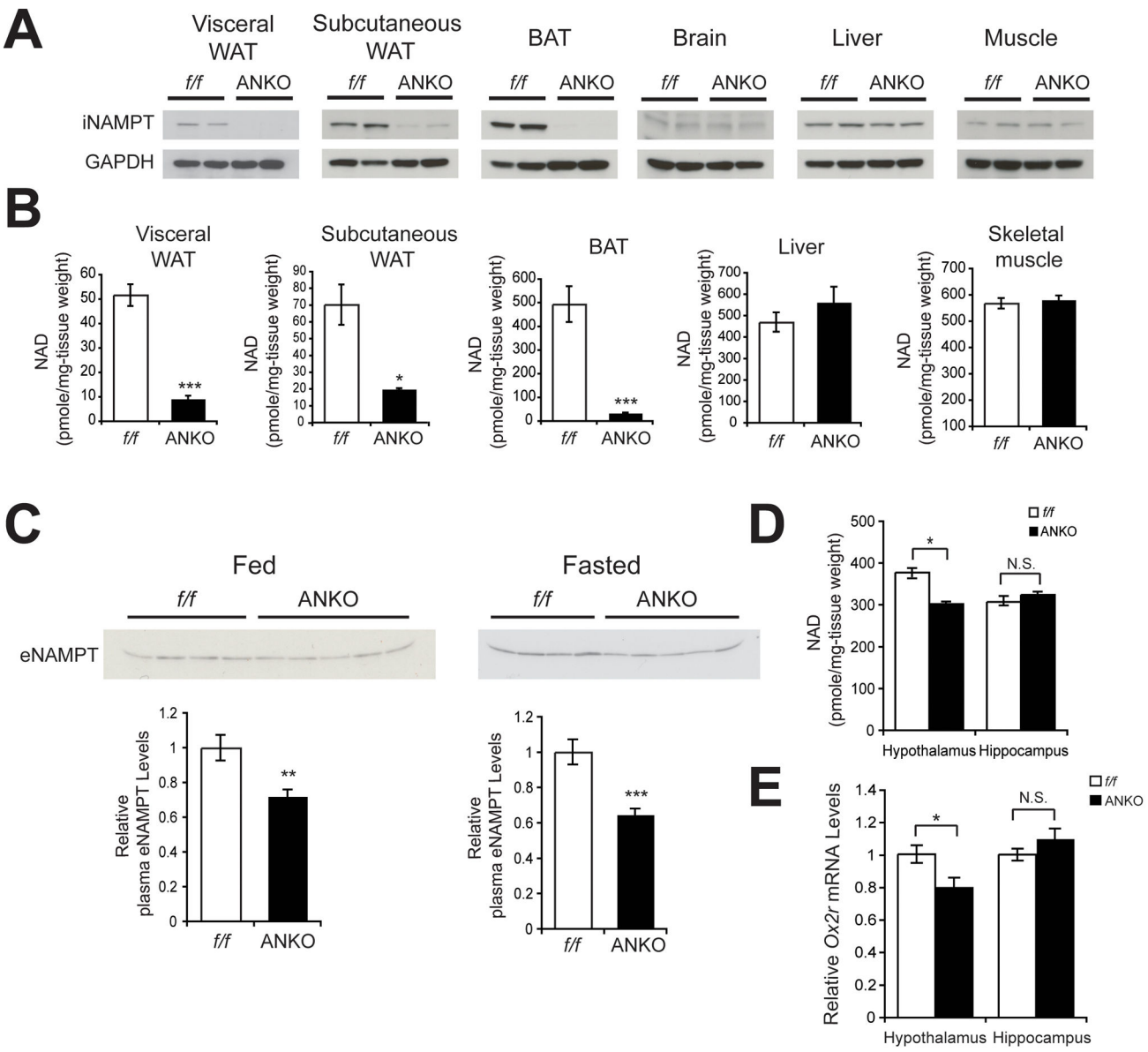

Figure 5.

ANKO mice exhibit reduced plasma eNAMPT levels and defects in NAD^+ biosynthesis not only in adipose tissue but also in the hypothalamus. **(A)** iNAMPT levels in visceral white adipose tissue (WAT), subcutaneous WAT, brown adipose tissue (BAT), brain, liver, and muscle from 2-month-old female *Nampt*$^{flox/flox}$ (*f/f*) and ANKO mice. **(B)** Tissue NAD^+ levels in visceral WAT, subcutaneous WAT, BAT, liver, and skeletal muscle from 3–4-month-old female *Nampt*$^{flox/flox}$ and ANKO mice (n=4–8). **(C)** Plasma eNAMPT levels in 5–6-month-old female *Nampt*$^{flox/flox}$ and ANKO mice. Plasma was collected from mice fed or fasted for 48 hr. Bottom panels show average plasma eNAMPT levels normalized to those of *Nampt*$^{flox/flox}$ mice (n=8–10). **(D)** Hypothalamic and hippocampal NAD^+ levels in 3–4-month-old female *Nampt*$^{flox/flox}$ and ANKO mice. (n=4–8) **(E)** Relative *Ox2r* mRNA expression levels in the hypothalami and the hippocampi from 3–4-month-old female

Nampt$^{flox/flox}$ and ANKO mice (n=4). Data in **B**–**E** were analyzed by the Student's *t* test. All values are presented as mean ± SEM. *p ≤ 0.05; **p ≤ 0.01; ***p ≤ 0.001.

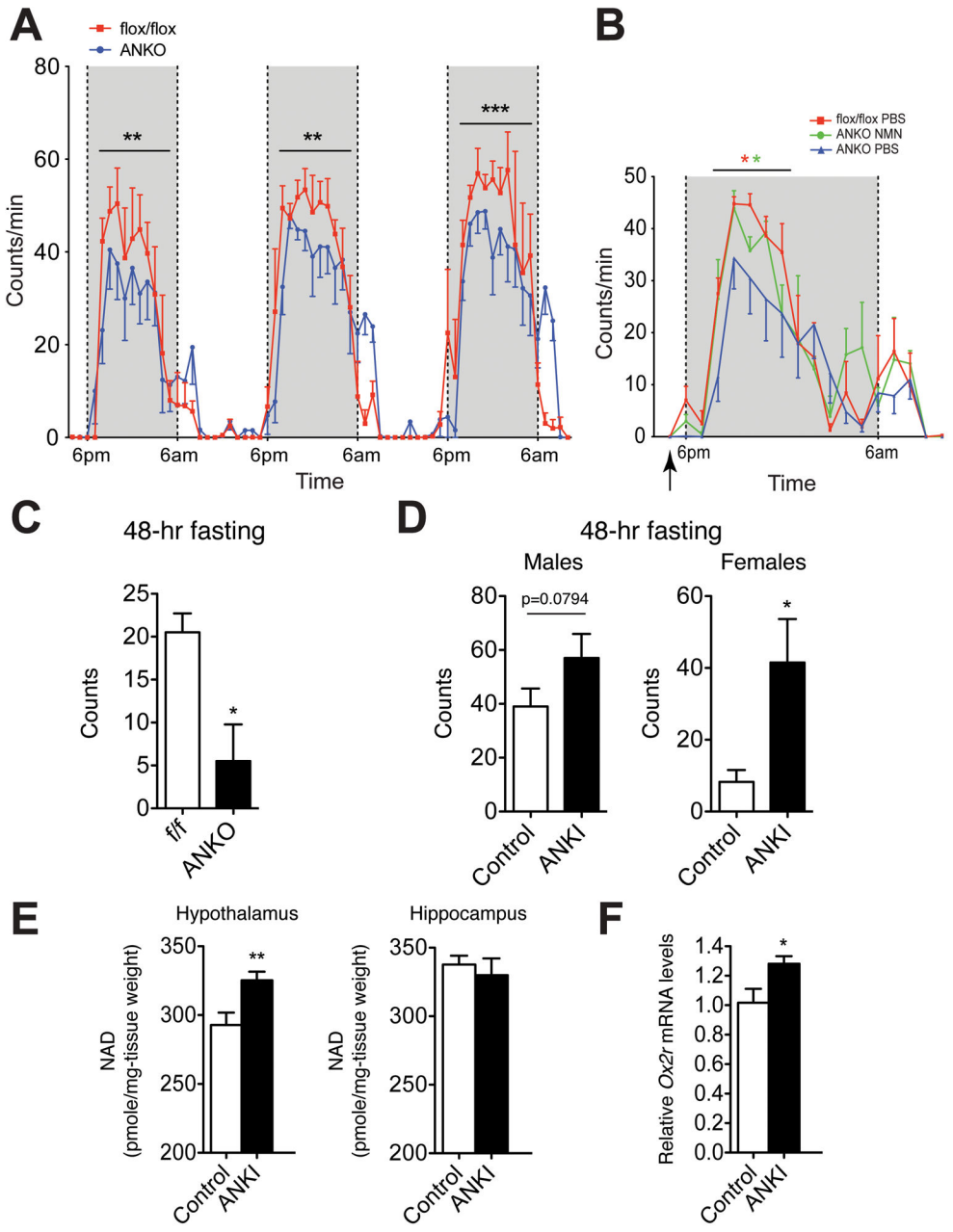

Figure 6.

Physical activity is altered in loss- and gain-of-function mouse models of adipose NAMPT. (**A**) Wheel-running activity of ANKO and *Nampt*$^{flox/flox}$ female mice at 5 months of age (n=3–6). (**B**) Wheel-running activity of NMN-injected ANKO female mice and PBS-injected ANKO and *Nampt*$^{flox/flox}$ female mice at 5 months of age (n=3–6). NMN was injected at 500 mg/kg body weight at 5pm (indicated by an arrow). Activity counts per minute at each time point are shown as mean values ± SEM. Data in **A** and **B** were analyzed by Wilcoxon matched-pairs singled-ranks test. (**C**) Physical activity levels (total numbers of quadrants crossed) measured after 48-hr fasting in ANKO and *Nampt*$^{flox/flox}$ female mice at 4–5 months of age (n=4). (**D**) Physical activity levels (total numbers of quadrants crossed)

measured after 48-hr fasting in ANKI and control male and female mice at 4–6 months of age (n=4). (**E**) Hypothalamic and hippocampal NAD^+ levels in 8–10 month-old ANKI and control male mice after 48-hr fasting (n=5). (**F**) Relative *Ox2r* mRNA expression levels in the hypothalami from 8–10 month-old ANKI and control male mice after 48-hr fasting (n=5). Data in **C**–**F** were analyzed by the Student's *t* test. All values are presented as mean ± SEM. *p ≤ 0.05; **p ≤ 0.01; ***p ≤ 0.001.

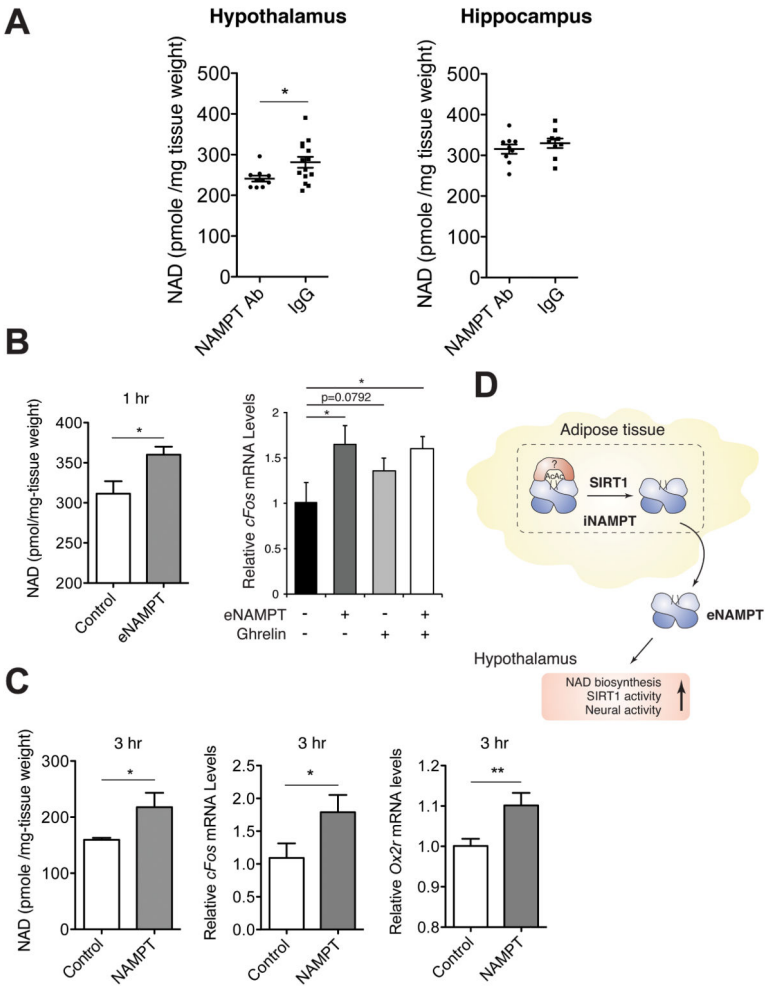

Figure 7.

eNAMPT regulates hypothalamic NAD$^+$ levels, *Ox2r* expression, and neural activation. (**A**) NAD$^+$ levels in the hypothalami and hippocampi isolated from B6 male mice after systemic injection of a NAMPT-neutralizing antibody. 20 μg of anti-NAMPT antibody (NAMPT Ab) and rabbit IgG (IgG) were injected into wild-type B6 male mice at 4–6 months of age. Hypothalamic NAD$^+$ levels 1 hr after injection were measured by HPLC (n=10–12). (**B**) NAD$^+$ levels (left) and *cFos* mRNA expression (right) in hypothalamic explants treated with eNAMPT-containing or control conditioned media. Hypothalamic explants prepared from female mice at 1–12 weeks of age were cultured in each conditioned medium for 1hr. For neural activity, ghrelin (10 μg/ml) and PBS were also added to eNAMPT-containing (+) or control- (−) conditioned media. NAD$^+$ levels were measured by HPLC, and *cFos* expression levels were quantitated by qRT-PCR (n=4–6). (**C**) NAD$^+$ levels and *cFos* and *Ox2r* mRNA expression in adult hypothalamic explants cultured in the media supplemented with the eNAMPT protein purified from HEK293 culture supernatants or bovine serum albumin (BSA) as a control for 3 hr (n=4–6). 1 μg of each protein was added to 50 μl of culture media containing a hypothalamic explant. Data were analyzed by the Student's *t* test or one-way ANOVA with Fisher's LSD *posthoc* test. All values are presented as mean ± SEM. *p

≤ 0.05; **p ≤ 0.01. (**D**) A model for the SIRT1-mediated regulation of eNAMPT secretion in adipose tissue. iNAMPT (a dimer in blue) is acetylated at lysine 53 (Ac), and SIRT1 specifically deacetylates this lysine, predisposing the protein to secretion. Acetyl-lysine 53 might provide a docking site to an unidentified factor (red) that prevents NAMPT from secretion. eNAMPT secreted from adipose tissue promotes NAD^+ biosynthesis, SIRT1 activity, and neural activity in the hypothalamus.